The allosteric mechanism of mTOR activation can inform bitopic inhibitor optimization

Yonglan Liu[a], Mingzhen Zhang[b], Hyunbum Jang[b] and Ruth Nussinov[b,c*]

[a]Cancer Innovation Laboratory, National Cancer Institute, Frederick, MD 21702, U.S.A.

[b]Computational Structural Biology Section, Frederick National Laboratory for Cancer Research, Frederick, MD 21702, U.S.A.

[c]Department of Human Molecular Genetics and Biochemistry, Sackler School of Medicine, Tel Aviv University, Tel Aviv 69978, Israel

Author for correspondence:

Tel: 301-846-5579

E-mail: NussinoR@mail.nih.gov

The authors declare no potential conflicts of interest.

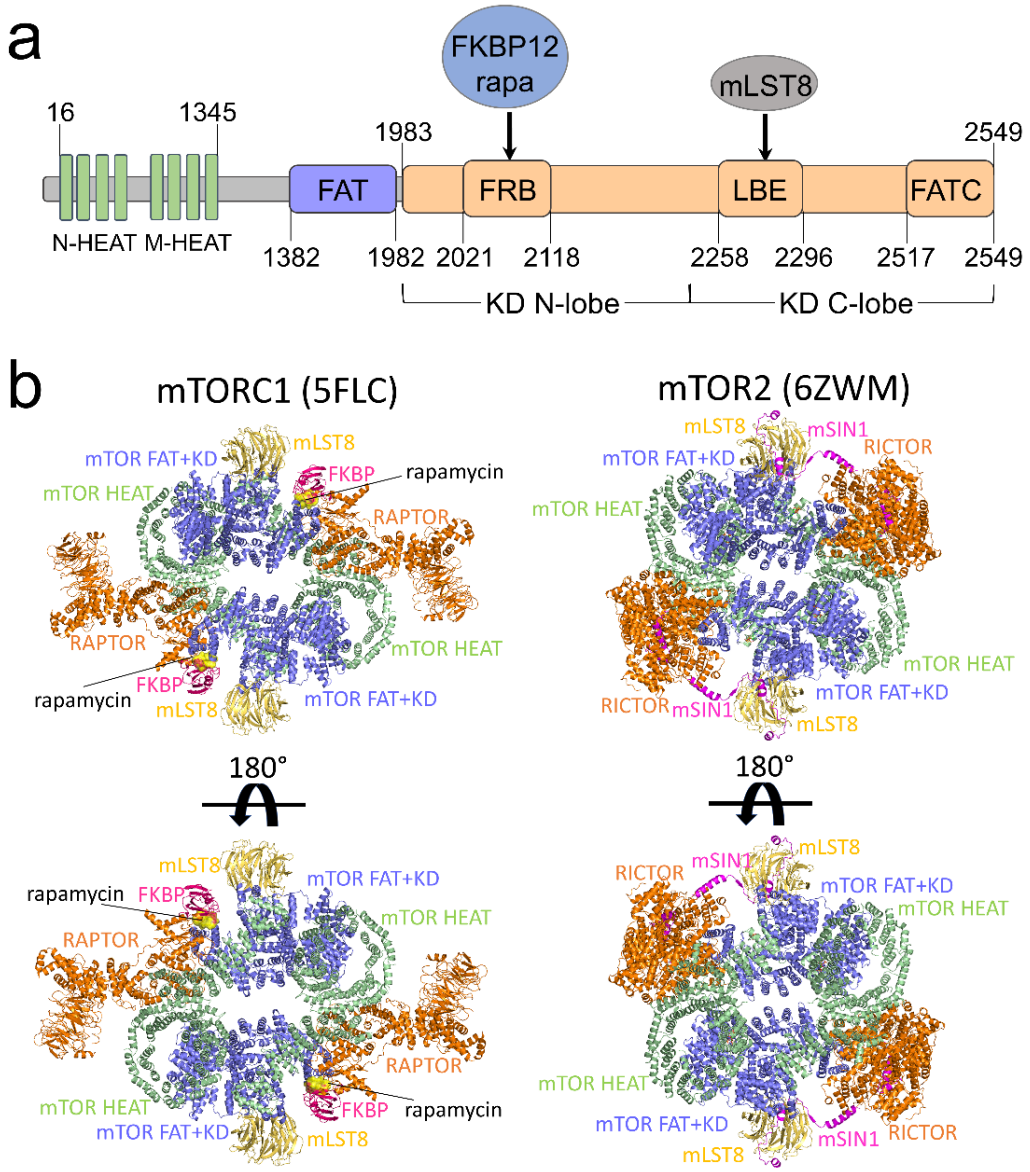

Fig. S1. (a) Domains of mTOR. It consists of the N-terminal HEAT repeats (residues 16-1345) including N-HEAT and M-HEAT, and the C-terminal FAT (residues 1382-1982) and the kinase (residues 1983-2549) domains. The kinase domain has three inserted domains, the FKBP12-rapamycin-binding (FRB, residues 2021-2118), Lst8 binding element (LBE, residues 2258-2296), and FAT C-terminal (FATC, residues 2517-2549) domains. The FRB and LBE domains are repsonsible for the binding of rapamycin-FKBP12 and mLST8, respectively. (b) The cryo-EM structures of mTORC1 (*left*, PDB ID: 5FLC) and mTORC2 (*right*, PDB ID: 6ZWM).

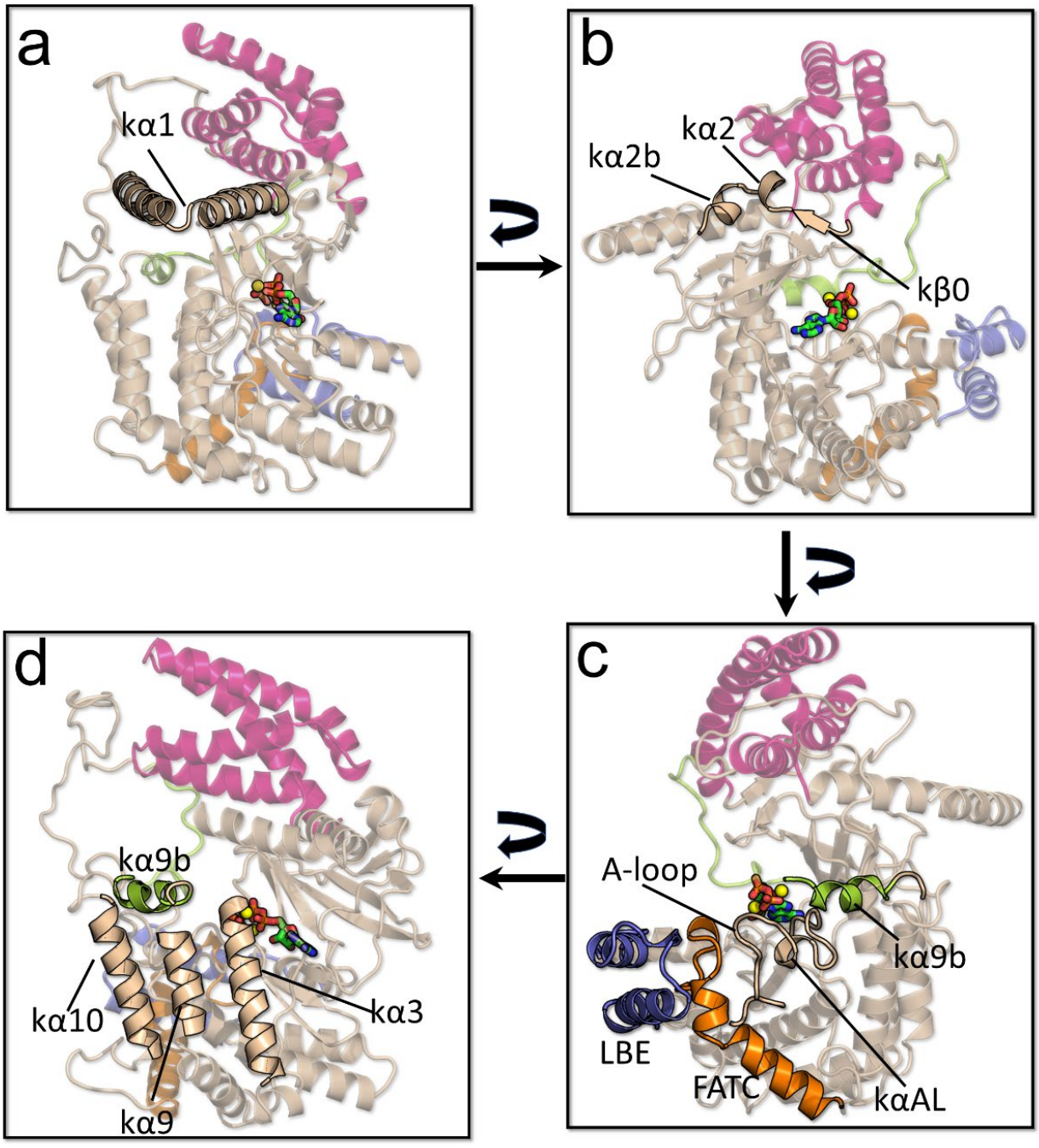

Fig. S2. Structural details of the mTOR kinase domain with highlights of (a) the kα1-helix, (b) the kα2-helix, the kα2b-helix, and the kβ0-strand, (c) the A-loop, the kα9b-helix, and the LBE and FATC domains, and (d) the kα3-helix, the kα9-helix, the kα9b-helix, and the kα10-helix.

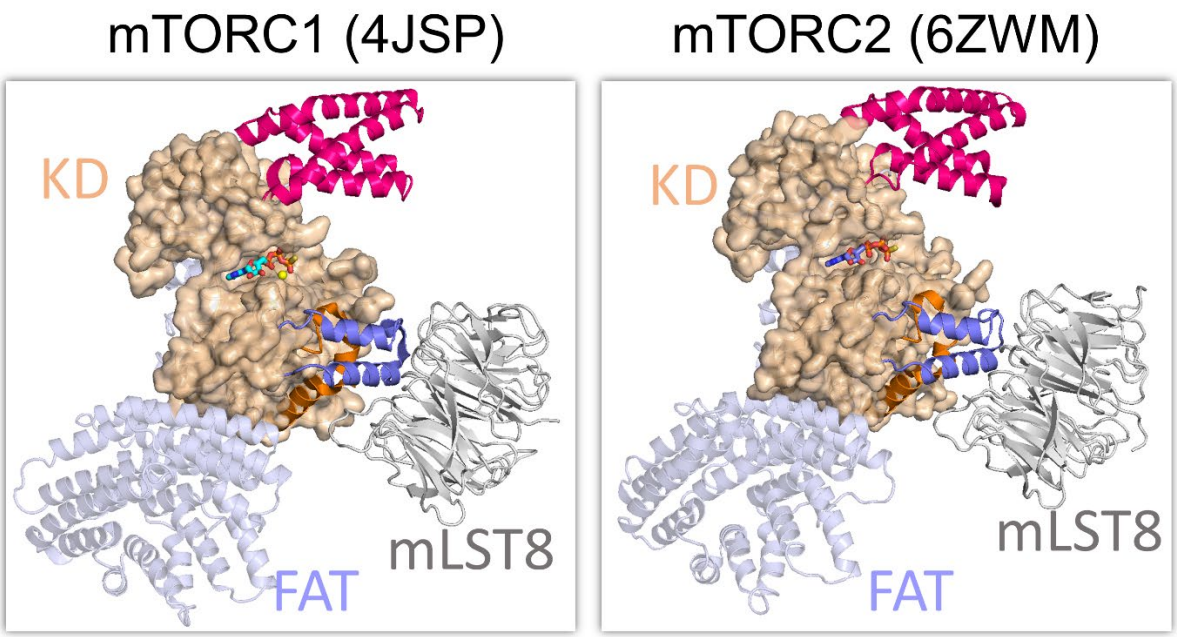

Fig. S3. Binding poses between mTOR and mLST8 of mTORC1 (*left*), and mTORC2 (*right*). These conformations are extracted from the crystal structures.

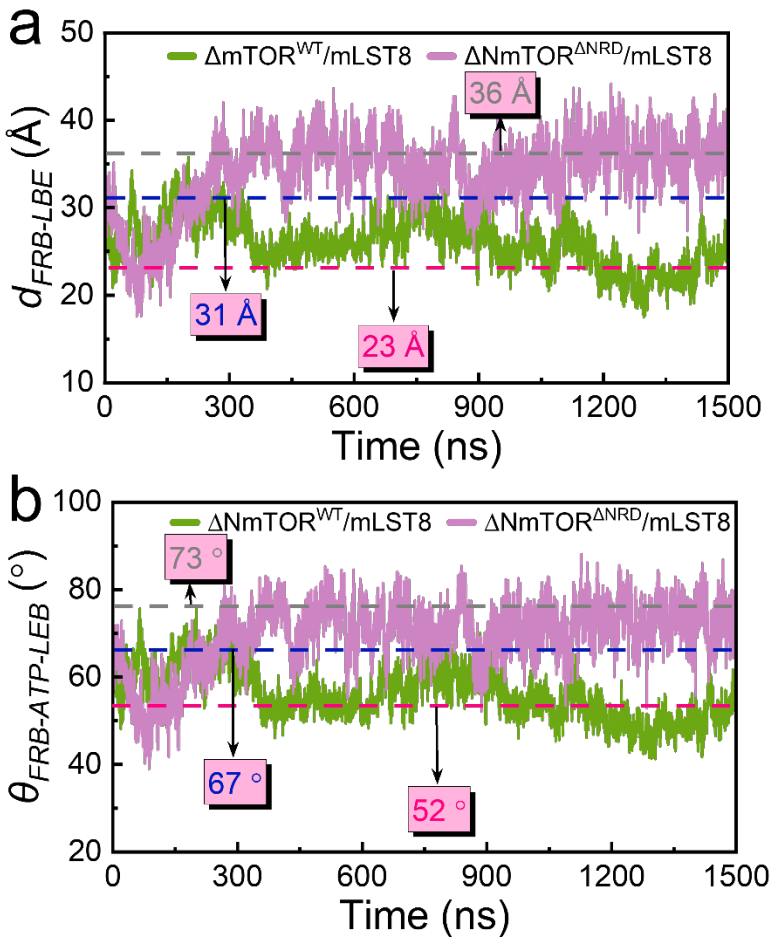

Fig. S4. Time-dependent (a) distances of FRB-LBE ($d_{FRB\text{-}LBE}$), and (b) angles of FRB-ATP-LBE ($\theta_{FRB\text{-}ATP\text{-}LBE}$). $d_{FRB\text{-}LBE}$ is the distance between the Cα atom of residue M2039 in the FRB domain and the Cα atom of residue M2277 in the LBE domain. $\theta_{FRB\text{-}ATP\text{-}LBE}$ is the angle between the vector from the phosphorus atom of the γ-phosphate of ATP to the Cα atom of residue M2039 in the FRB domain and the vector from the phosphorus atom of the γ-phosphate of ATP to the Cα atom of residue M2277 in the LBE domain. $d_{FRB\text{-}LBE}$ and $\theta_{FRB\text{-}ATP\text{-}LEB}$ in the crystal structure of ΔNmTOR/mLST8 (~31 Å and ~67°, blue dash lines) are marked out in (a) and (b), respectively. $d_{FRB\text{-}LBE}$ and $\theta_{FRB\text{-}ATP\text{-}LEB}$ that the simulated systems of ΔNmTOR^{WT}/mLST8 (~23 Å and ~52°, hot-pink dash lines) and ΔNmTOR$^{\Delta NRD}$/mLST8 (~36 Å and ~73°, gray dash lines) populate are also highlighted in (a) and (b), respectively.

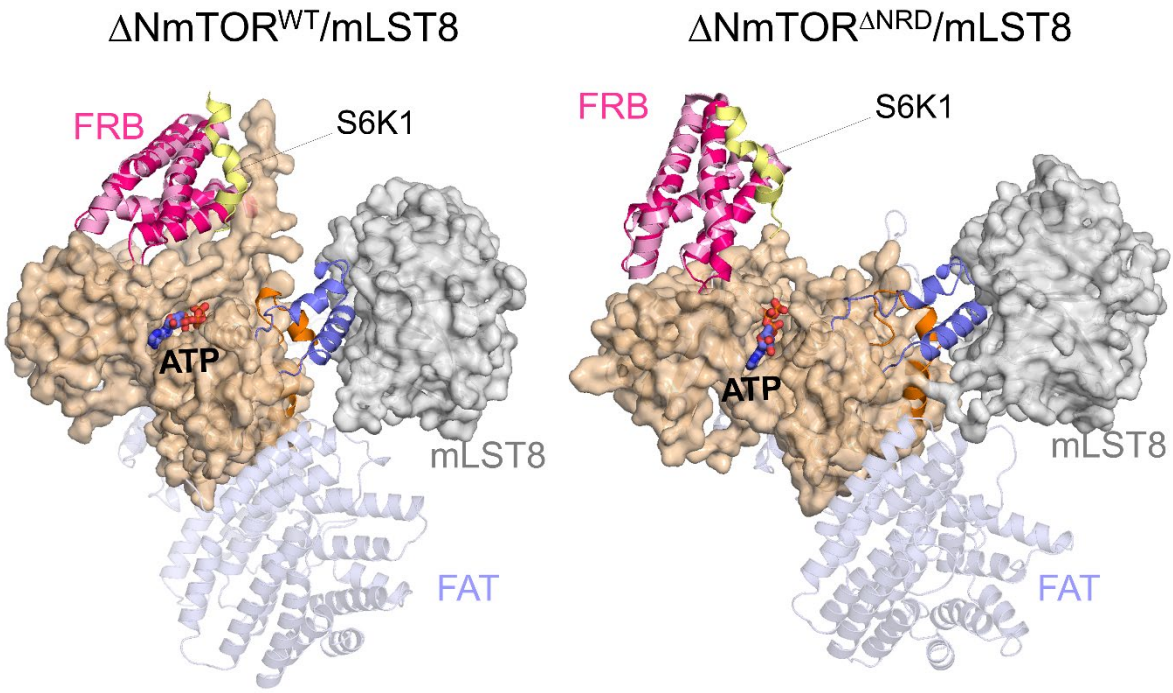

Fig. S5. Snapshots to present the binding of a mTORC1 substrate (S6K1) and the FRB domain of mTOR in ΔNmTOR^{WT}/mLST8 and ΔNmTOR$^{\Delta NRD}$/mLST8. The binding poses between the substrate and FRB is through aligning the crystal structure of the FRB/S6K1 complex (PDB ID: 5WBH) to the final configurations of the mTOR FRB domain.

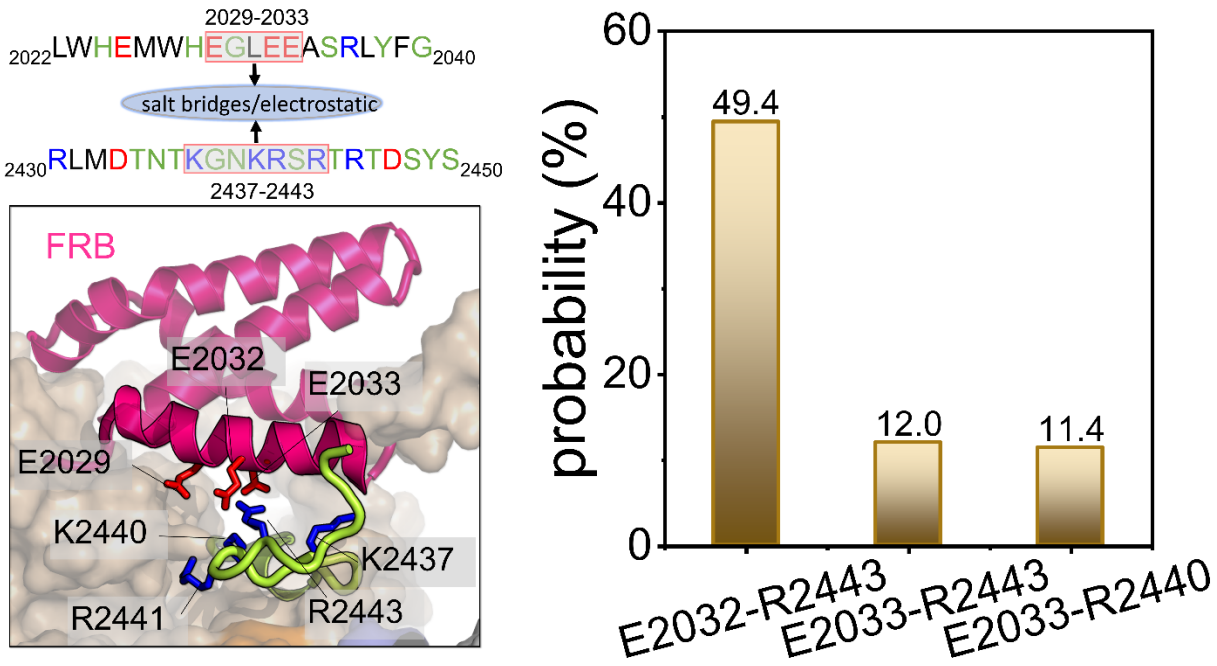

Fig. S6. A snapshot representing the interaction between NRD (residues 2430-2450) and the FRB helix (residues 2022-2040), and the probability of the salt bridges (E2032-R2443, E2033-R2443, and E2033-R2440) formed between some positive charged residues in NRD and negative charged residues (E2032 and E2033) in the FRB helix for the ΔNmTOR^{WT}/mLST8 system. Data in the probability were extracted from the last 500-ns trajectories.

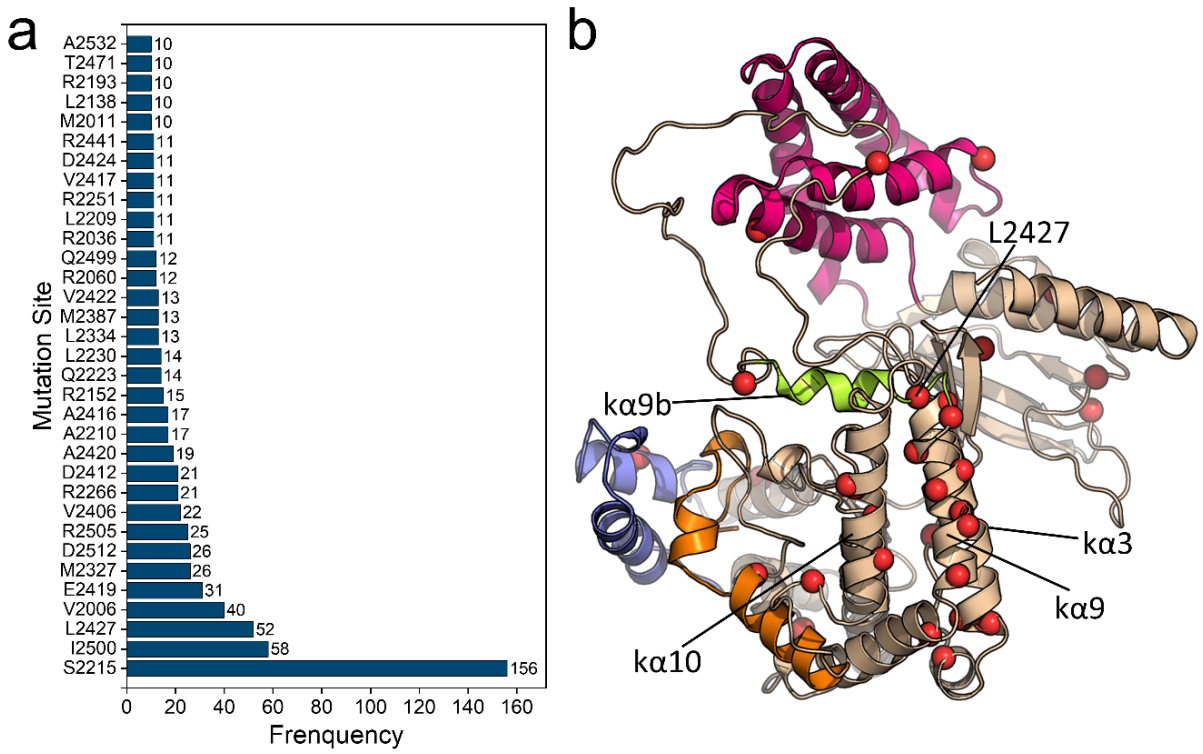

Fig. S7. (a) Statistics of mTOR-activating mutations in the kinase domain with frequency ≥ 10. (b) These mutations are mapped to the structure of the mTOR kinase domain. The statistical data in (a) was extracted from the combination of the TCGA, GENIE, and COSMIC databases. Helices kα3, kα9, kα9b, and kα10, as well as the L2427 residue, are marked out.

Table S1. Details of simulation systems.

system name	components	mTOR mutation	No. of parallel trajectories	simulation time
ΔNmTOR^{WT}/mLST8	ΔNmTOR, mLST8, ATP, 2 Mg^{2+}	/	3	1500 ns
ΔNmTOR$^{\Delta NRD}$/mLST8	ΔNmTOR, mLST8, ATP, 2 Mg^{2+}	2430-2450 deletion	3	1500 ns
ΔNmTOR^{L2427R}/mLST8	ΔNmTOR, mLST8, ATP, 2 Mg^{2+}	L2427R mutation	3	1500 ns